Oblique-Roll Electrohydrodynamic Instability in Nematics

Walter Zimmermann and Lorenz Kramer
Physikalisches Institut der Universität Bayreuth, 8580 Bayreuth, Federal Republic of Germany
(Received 22 March 1985)

A three-dimensional analysis of the electrohydrodynamic instability in a planar oriented nematic liquid crystal with stress-free boundary conditions shows that for appropriate, realistic parameters of materials like MBBA and PAA the instability sets in for a periodic roll structure that is oblique with respect to the undisturbed director $\hat{\mathbf{n}}$. By a change in the frequency and/or application of a magnetic field, a continuous transition from perpendicular to oblique rolls can be induced. We analyze the mechanism, discuss the possible influence of nonlinearities, and compare with experiments.

PACS numbers: 61.30.Gd, 05.70.Ln, 47.20.+m, 47.65.+a

When a low-frequency alternating voltage is applied across a thin layer of nematic liquid crystal having negative (or slightly positive) dielectric anisotropy, sufficient (ionic) conductivity, and uniform orientation of the director $\hat{\mathbf{n}}$ in the plane of the layer, an electrohydrodynamic instability (EHI) which leads to a periodic pattern of convection rolls occurs (for reviews see Gossens and Blinov[1,2]). In this system the director, which is oriented at the upper and lower plate by appropriate boundary conditions, defines a preferred axis within the plane of the layer. The periodic structure is expected to orient itself in a definite way with respect to $\hat{\mathbf{n}}$. All theoretical investigations in the past have started from the assumption that the rolls are perpendicular to the undisturbed director (two-dimensional Williams domains), and this structure was reported from experiments.[1,2] Recently, however, Ribotta, Joets, and Lei[3] observed a direct transition into a state with oblique rolls below a critical frequency ω_z. Above ω_z the first transition to perpendicular rolls was followed by a transition to an undulated structure. Further increase of voltage led to oblique rolls.

In the well-known Rayleigh-Bénard instability of simple fluids[4] the orientation of the rolls is, apart from lateral boundary effects, arbitrary. The situation in the EHI of neumatic liquid crystals is similar to Rayleigh-Bénard convection in a conducting fluid in the presence of a horizontal magnetic field, where convection sets in with the rolls along the magnetic field.[5] When the layer is in addition rotating, the convection rolls make an acute angle with the direction of a sufficiently large magnetic field.[6] Actually our problem is also similar to Taylor vortex flow, especially in the small-gap limit (preferred axis = cylinder axis). There, spiral vortex structures (the analog of oblique rolls) may occur for counter-rotating cylinders.[7,8]

Here we present a three-dimensional linear analysis of the EHI which determines the structure at threshold up to degeneracies. Consider a nematic slab [Fig. 1(a)] with the undistorted director $\hat{\mathbf{n}}$ in the x direction and applied voltage $V(t)$ between the plates. We start from the general electrohydrodynamic equations,[1,9] introduce spherical polar coordinates for the director $\hat{\mathbf{n}} = (\cos\theta\cos\psi, \cos\theta\sin\psi, \sin\theta)$, and linearize around the undistorted state (see, e.g., Appendix A of Manneville and Dubois-Violette[10]). By elimination of the pressure and the charge density one obtains six coupled linear partial differential equations for the velocity components v_i, $i = 1,2,3$, the potential φ of the induced electric fields, and the angles θ and ψ of the director distortion.

We consider an alternating voltage $V = (V_0/\sqrt{2})\cos\omega t$. At threshold (marginal-stability point) we expect that nontrivial ω-periodic solutions exist (steady bifurcation or exchange of stability). All quantities may then be expanded in a Fourier series. In the low-frequency or conduction regime[11] a meaningful approximation is obtained by keeping only the time-independent components (averages) for the director and velocities, and the fundamental component

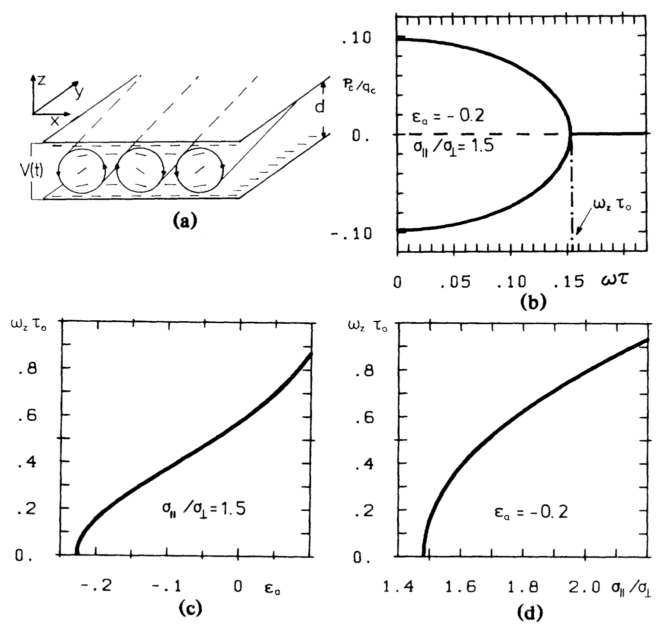

FIG. 1. (a) Sketch of the periodic convection structure. (b) The pitchfork bifurcation in the p_c/p_c-$\omega\tau_0$ plane for MBBA. (c),(d) The dependence of the critical frequency ω_z on ϵ_a and $\sigma_\parallel/\sigma_\perp$.

$\varphi=\varphi_1\cos\omega t+\varphi_2\sin\omega t$ for the potential.[11-14] This approximation is for conductivities σ of the nematic material and layer thicknesses d with $\sigma d^2 \gtrsim 10^{-17}\ \Omega^{-1}$ m valid over most of the conduction regime.[12,14] The resulting equations become fully algebraic with the *Ansatz*

$$\begin{aligned} v_{x,y}&=A_{1,2}\sin z\cos(qx+py),\\ v_z&=A_3\cos z\sin(qx+py),\\ \varphi_{1,2}&=A_{4,5}\cos z\sin(qx+py),\\ \theta&=A_6\cos z\cos(qx+py),\\ \psi&=A_7\sin z\sin(qx+py). \end{aligned}\tag{1}$$

Here all lengths are measured in units of π/d so that $|z|\leq\pi/2$. Clearly v_x, v_y, and ψ are not zero at the boundaries, and the boundary conditions indeed correspond to an unrealistic stress-free surface. This deficiency of the theory could in principle be fixed by superposing degenerate harmonic modes as first done by Penz and Ford,[9] or by choosing the *Ansatz* (1) only for the x and y directions and integrating numerically with respect to z. In both cases no analytic expression for the threshold can be obtained, and we therefore continue with the solutions (1). As in the two-dimensional case this simplification preserves all qualitative features.[9,13,14]

The resulting system of homogeneous linear equations for the A_i is solvable only if the determinant vanishes and this gives the following expression for the threshold voltage V_0 as a function of q, p, ω, material parameters, and applied magnetic fields:

$$V_0^2=\frac{\pi^2(1+\omega^2\tau^2)[K_2-p^2(k_{11}-k_{22})^2/K_1]}{\epsilon_a\epsilon_0[q^2(\sigma_a\epsilon_\perp D/\epsilon_a\sigma_\perp S-1)M+D^{-1}(q^2+P)(DS^{-1}+\omega^2\tau^2)]},\tag{2}$$

where

$$K_1=k_{11}p^2+k_{22}+k_{33}q^2+d^2\chi_a\mu_0(H_x^2-H_y^2)/\pi^2,\quad K_2=k_{11}+k_{22}p^2+k_{33}q^2+d^2\chi_a\mu_0(H_x^2-H_z^2)/\pi^2,$$

$$S=q^2\sigma_\parallel/\sigma_\perp+P,\quad D=q^2\epsilon_\parallel/\epsilon_\perp+P,\quad P=1+p^2,\quad \tau=\tau_0 D/S,\quad \tau_0=\epsilon_0\epsilon_\perp/\sigma_\perp,\tag{3}$$

$$M=\{p^2[(\alpha_3p^2-\alpha_2q^2)\beta_1-\alpha_3\beta_2](k_{11}-k_{22})/K_1+[-\alpha_3\beta_1p^2+(\alpha_3-\alpha_2q^2)\beta_2]\}/(\beta_2\beta_3-\beta_1^2p^2),\tag{4}$$

$$\beta_1=\beta-\tfrac{1}{2}\alpha_4q^2,\quad \beta=\eta_2P+(\eta_1+\eta_2+\alpha_1)q^2,\quad \beta_2=\tfrac{1}{2}\alpha_4q^2+\beta p^2+\eta_1q^4,\quad \beta_3=\beta+\tfrac{1}{2}\alpha_4q^2p^2+\eta_1q^4.\tag{5}$$

The viscosities $\alpha_1,\ldots,\alpha_6$ and $\eta_1=(\alpha_4+\alpha_5-\alpha_2)/2$, $\eta_2=(\alpha_3+\alpha_4+\alpha_6)/2$ as well as the elasticities k_{11}, k_{22}, k_{33} are defined as usual (see, e.g., Refs. 1 and 2), and $\epsilon_a=\epsilon_\parallel-\epsilon_\perp$, $\sigma_a=\sigma_\parallel-\sigma_\perp$ are the anisotropies of the dielectric constant and of the conductivity (the dielectric and conductivity tensors are, respectively, $\epsilon_{ik}=\epsilon_\perp\delta_{ik}+\epsilon_a n_i n_k$ and $\sigma_{ik}=\sigma_\perp\delta_{ik}+\sigma_a n_i n_k$). Equation (2) was derived for the case where at most one of the components of the magnetic field $\mathbf{H}=(H_x,H_y,H_z)$ is nonzero. For $p=0$ the results for the two-dimensional analysis are recovered.[1,13]

In the relevant parameter range the curve V_0 (q, $p=0$) has a minimum V_{c2} (two-dimensional threshold) at the critical wave number q_c corresponding to perpendicular rolls. V_{c2} is a minimum with respect to variations of p as long as $\partial^2V_0/\partial^2p>0$ at $|q|=q_c$, $p=p_c=0$. Otherwise there exists a lower threshold V_{c3} for $|p|=p_c>0$. Inserting standard values for the material parameters of N-[p-methoxybenzylidine]-p-butylaniline (MBBA) (see Table I)[2] except for ϵ_a, which we allow to vary keeping the angular average $\bar{\epsilon}=(2\epsilon_\perp+\epsilon_\parallel)/3=4.92$ fixed, one finds $p_c=0$ for $\epsilon_a<-0.226$ and $p_c>0$ for $-0.226<\epsilon_a\lesssim 0.38$ at $\omega=0$ and $\mathbf{H}=0$. For $\epsilon_a\gtrsim 0.38$ the threshold for the electric Fréedericksz transition $V_F^2=\pi^2k_{11}/\epsilon_a\epsilon_0$ [$q=p=0$ in Eq. (2)] becomes lower.

The oblique-roll structure can always be suppressed by an increase of the frequency ω beyond a critical value ω_z. In Fig. 1(b) the values for p_c/q_c are plotted as a function of $\omega\tau_0$ [see Eq. (3)] for $\epsilon_a=-0.2$ (Ribotta, Joets, and Lei[3] quote this value for their experiments on MBBA). At ω_z there is the typical pitchfork bifurcation which we always find for the transitions to the oblique-roll state. The vertical slope of $p_c(\omega)$ at ω_c has apparently not been observed.[15] Possibly lateral boundaries disturb the effect slightly above threshold. Our theory gives $\omega_z/2\pi=5.25\ \mathrm{s}^{-1}$ for $\epsilon_a=-0.2$, $\sigma_\perp=1.2\times10^{-8}\ \Omega^{-1}\ \mathrm{m}^{-1}$ ($\sigma_\perp$ was estimated by fitting the theoretical cutoff frequency to the experiment[3]) and standard values of MBBA. The discrepancy with the measured value $\omega_z/2\pi\approx 40\ \mathrm{s}^{-1}$ is due either to the approximations made in our theory (mainly unrealistic boundary conditions) or to deviations of the material constants from the standard values used. In Figs. 1(c) and 1(d) the variation of ω_z with ϵ_a and with $\sigma_\parallel/\sigma_\perp$ are shown. These parameters can be varied by addition of appropriate guest molecules to the host material.[2] Our results are consistent with the fact that in most experiments on MBBA perpendicular rolls are found (usually $\epsilon_a\approx-0.5$).

If ϵ_a is chosen not too far below -0.226, the transition from perpendicular to oblique rolls can be induced by varying any one of the material parameters. In

TABLE I. In the *second column* standard values for material parameters of MBBA, as in Ref. 2 (except for ϵ_a), are given (elasticities in units 10^{-12} N and viscosities in units 10^{-3} kg m^{-1} s^{-1}). At those values the transition to perpendicular rolls takes place at $V_0 = V_{c2} = 5.67$ V and critical wave number $q_c = 1.250$ ($\omega = H_i = 0$ throughout). When any one of the parameters is varied alone a transition to oblique rolls occurs at the value in the *third column*. In the *fourth* and *fifth columns* the corresponding changes of the threshold voltage and critical wave number are given.

Material parameters	Standard values	Transition values	(Change of V_{c2}) $\times 10^2$	(Change of q_c) $\times 10^3$
k_{11}	6.1	6.3	3.7	6.3
k_{22}	4.0	3.9	0.0	0.0
k_{33}	7.25	8.06	20.1	−17.4
α_1	6.5	9.5	3.8	6.8
α_2	−77.5	−83.9	−20.7	−15.5
α_3	−1.2	−12.9	26.1	88.6
α_4	83.0	77.7	−14.3	−17.5
α_5	46.0	55.8	15.9	3.0
α_6	−35.0	−27.4	7.8	21.4
$\epsilon_\parallel$	4.72	6.32	−87.1	−45.8
ϵ_a	−0.3	−0.226	−14.5	−45.9
$\sigma_\parallel$	1.5	1.55	−25	−21

Table I the transition values for each parameter are given (all others kept fixed) for $\epsilon_a = -0.3$ and $\omega = 0$. We have also included the change in the threshold voltage and the change in q_c. The material constants for p,p'-azoxydianisole (PAA)[2] are such that the oblique rolls should occur in a large range of ϵ_a.

Although it is not easy to understand all the trends in terms of simple physical ideas, we provide some discussion of various influences. The Carr-Helfrich mechanism,[16,17] which drives the "anomalous" alignment of the director in the perpendicular-roll instability, is also responsible for the transition to oblique rolls. Thus spatial variations of the director in the presence of an external electric field lead to a charge density

$$\rho = \frac{\pi V_0 \epsilon_0}{\sqrt{2} d} q (\sigma_a \epsilon_\perp - \epsilon_a \sigma_\perp) \frac{q^2 + P}{\sigma_\parallel q^2 + \sigma_\perp P} \theta \qquad (6)$$

(independent of ψ). Equation (6) follows from charge conservation $\nabla_i(\sigma_{ik} E_k) + \dot{\rho} = 0$ ($\mathbf{E}$ = total electric field) and Coulomb's law $\nabla_i(\epsilon_{ik} E_k) = \rho$ for small, periodic variations of θ in the static limit. The electric field in the charged fluid now initiates hydrodynamic flow which in turn acts back on the director. This feedback is positive for $\sigma_a \epsilon_\perp - \epsilon_a \sigma_\perp > 0$, and so spatial variations of $\hat{\mathbf{n}}$ (and all other quantities) appear spontaneously above threshold. Equation (6) shows that for $\sigma_\parallel / \sigma_\perp > 1$ and given amplitude of θ, the charge density increases with increasing p^2. This provides the driving force for the oblique-roll instability. Clearly large values of $\sigma_\parallel / \sigma_\perp$ favor the effect.

The buildup of the charge distribution is governed by the charge relaxation time τ, and so the dominant effect of ω is to increase the threshold V_0 with $\omega^2 \tau^2$. Since τ increases with p^2, oblique rolls are for increasing ω more and more suppressed.

For $q^2 >> 1$ spatial variations in the z direction become negligible. Then a one-dimensional description of the Williams domains, which has been used extensively in the past, becomes possible.[11,17,18] In this approximation the oblique-roll instability does not occur, because q^2 and p^2 enter in many places in Eqs. (2)–(5) additively, so that for decreasing q^2 nonzero values of p^2 become more favorable (keeping all other quantities fixed). Actually this behavior is quite general and is related to the mechanism leading to the zigzag instability in Rayleigh-Bénard convection.[4]

When ϵ_a increases, both V_{c2} and q_c decrease (the latter is very pronounced; see Table I), because the homogeneous stabilizing effect of the electric field is reduced. The positive effect of increasing ϵ_a on the oblique-roll structure is a result of the decreasing q^2, whereas the direct effect of increasing ϵ_a, keeping q^2 fixed, is in fact opposite.

A magnetic field H_x in the x direction raises V_{c2} and q_c and suppresses the oblique rolls, whereas the opposite is true for a field H_z in the z direction (for $\chi_a > 0$). Both effects are similar to the effect of changing ϵ_a and are again explained by the variation of q^2. A finite magnetic field H_y destabilizes the director in the x-z plane and therefore favors oblique rolls.

In the oblique-roll state one has a twist deformation in contrast to perpendicular rolls. Therefore a sufficiently small twist elasticity k_{22} is essential for oblique rolls. Both splay and bend deformation are relieved by the twisting, so that large values of k_{11} and k_{33} relative to k_{22} are favorable for oblique rolls.

The viscosities act in different ways on the instability. It is useful to recall the role of the shear viscosities $\eta_1, \eta_2, \eta_3 = \alpha_4/2$ and α_1, and of the rotational viscosities $\gamma_{1,2} = \alpha_3 \pm \alpha_2$ (see, e.g., Refs. 1 and 18), which couple the hydrodynamic motion with the viscous torque $\mathbf{\Gamma}$ on the director. For perpendicular rolls only η_1, η_2, and α_1 describe the friction of the hydrodynamic flow. Increasing η_1, η_2, and α_1 with respect to η_3 favors flow out of the x-z plane, and therefore oblique rolls. This explains the influences of α_1, α_2, α_4, α_5, and α_6 as shown in Table I. Decreasing α_2 or α_3 increases Γ_z, which promotes orientation of the director out of the x-z plane (for α_2 this is consistent with the influence through η_1). Decreasing α_2 (or α_3) increases (or decreases) Γ_y, which decreases (or increases) V_{c2}.

Let us now discuss the influence of nonlinearities above threshold. Their immediate effect is to fix the amplitude of the structure and to select among linearly degenerate structures. Besides the oblique rolls, which we chose in Eq. (1), one could also have rectangular cells, which are obtained as a superposition of rolls with positive and negative p. These features can be reproduced by simple two-dimensional anisotropic models.[19] In addition one finds in the nonlinear regime of such models undulated rolls, as observed by Ribotta, Joets, and Lei.[3]

We hope that our results will stimulate more experiments in this field and lead to more quantitative comparisons. We are now calculating the threshold curves for rigid boundary conditions and with corrections to the frequency expansion. Moreover, we plan to investigate the nonlinear behavior slightly above threshold including wavelength selection properties as done for other systems.[20,21]

We are grateful to R. Ribotta for calling our attention to this problem and to E. Bodenschatz, F. H. Busse, W. Pesch, and R. Ribotta for very helpful discussions. This work was supported by the Deutsche Forschungsgemeinschaft (Sonderforschungsbereich 213, Bayreuth).

[1]W. J. A. Goossens, in *Advances in Liquid Crystals,* edited by G. H. Brown (Academic, New York, 1978), Vol. 3, p. 1.

[2]L. M. Blinov, *Electro-Optical and Magneto-Optical Properties of Liquid Crystals* (Wiley, New York, 1983).

[3]R. Ribotta, A. Joets, and Lin Lei, to be published; A. Joets and R. Ribotta, in *Cellular Structures in Instabilities,* edited by J. E. Wesfreid and S. Zaleski (Springer, New York, 1984), p. 294.

[4]F. H. Busse, in *Hydrodynamic Instabilities and the Transition to Turbulence* (Springer-Verlag, Berlin, 1981).

[5]S. Chandrasekhar, *Hydrodynamic and Hydrodynamic Stability* (Clarendon, Oxford, England, 1961), p. 186.

[6]I. A. Eltayeb, Proc. Roy. Soc. London, Ser. A **326**, 229 (1972).

[7]E. R. Krüger, A. Gross, and R. C. DiPrima, J. Fluid Mech. **24**, 521 (1966).

[8]H. A. Snyder, Int. J. Non-Linear Mech. **5**, 659 (1970).

[9]P. A. Penz and G. W. Ford, Phys. Rev. A **6**, 414 (1972).

[10]P. Manneville and E. Dubois-Violette, J. Phys. (Paris) **37**, 285 (1976).

[11]E. Dubois-Violette, P. G. de Gennes, and O. Parodi, J. Phys. (Paris) **32**, 305 (1971).

[12]P. Sengupta and A. Saupe, Phys. Rev. A **9**, 2698 (1974).

[13]D. Meyerhofer, in *Introduction to Liquid Crystals,* edited by E. B. Priestly, P. J. Wojtowicz, and Ping Sheng (Plenum, New York, 1975); V. G. Chigrinov and S. A. Pikin, Kristallografiya **23**, 333 (1978) [Sov. Phys. Crystallogr. **22**, 184 (1978)].

[14]E. Bodenschatz, W. Zimmermann, and L. Kramer, unpublished.

[15]R. Ribotta, private communication.

[16]E. F. Carr, Mol. Cryst. Liq. Cryst. **7**, 253 (1969).

[17]W. Helfrich, J. Chem. Phys. **51**, 4092 (1969).

[18]P. G. de Gennes, *The Physics of Liquid Crystals* (Clarendon, Oxford, England, 1974), p. 166.

[19]W. Pesch and L. Kramer, unpublished.

[20]W. Zimmermann and L. Kramer, J. Phys. (Paris) **46**, 343 (1985).

[21]L. Kramer and H. Riecke, Z. Phys. **59**, 245 (1985).